

SUPPLEMENTAL INFORMATION

Figure S1, Related to Figure 1.

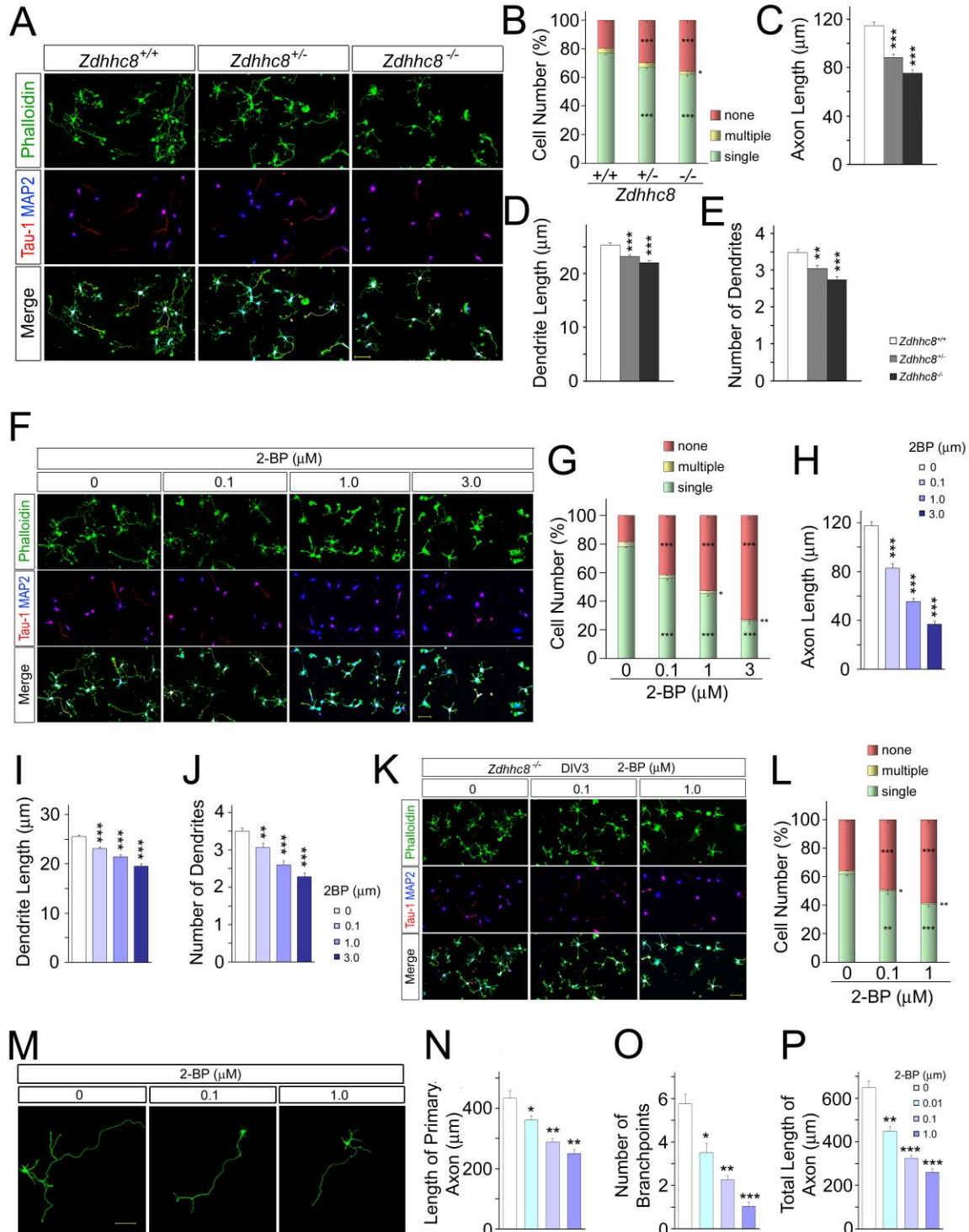


Figure S1, Related to Figure 1. Axonal alterations in *Zdhhc8*-deficient cortical neurons.

(A) Deficits of neuronal polarity in *Zdhhc8*-deficient cortical neurons at DIV3. Cortical neurons were immunostained with Tau-1 (*red*), MAP2 (*blue*), and phalloidin (*green*). Scale bar, 50 μm

(B) Quantification of neurons, having a single (*green*), multiple (*yellow*), or none (*pink*) Tau-1-positive process in *Zdhhc8*-deficient cortical cultures. 12 areas (>100 neurons/area) were analyzed for each genotype.

(C-E) Quantification of axon length, dendrite length, and dendrite number in *Zdhhc8*-deficient cortical neurons (> 200 neurons per each genotype).

(F) Effect of 2-BP on neuronal polarity of WT cortical neurons at DIV3. 2-BP was added at 3 hrs following inoculation and cells were fixed at DIV3. Neurons were immunostained with Tau-1 (*red*), MAP2 (*blue*), and phalloidin (*green*). Scale bar, 50 μm .

(G) Quantification of neurons, having a single (*green*), multiple (*yellow*), or none (*pink*) Tau-1-positive process in WT cortical cultures treated with 2-BP. 12 areas (>100 neurons/area) were analyzed for each concentration of 2-BP.

(H-J) Quantification of axon length, dendrite length, and dendrite number in WT cortical neurons treated with 2-BP (> 200 neurons per each concentration of 2-BP).

(K) Effect of 2-BP on polarity of *Zdhhc8*^{-/-} cortical neurons. 2-BP was added at 3 hrs following inoculation and cells were fixed at DIV3. Neurons were immunostained with Tau-1 (*red*), MAP2 (*blue*), and phalloidin (*green*). Scale bar, 50 μm .

(L) Quantification of neurons, having a single (*green*), multiple (*yellow*), or none (*pink*) Tau-1-positive process in *Zdhhc8*^{-/-} cortical cultures. 12 areas (>100 neurons/area) were analyzed for each concentration of 2-BP

(M) Representative images of palmitoylation-dependent axonal deficits in cortical neuron *in vitro*. Cortical neurons were transfected with EGFP constructs, treated with various concentrations of 2-BP and fixed at DIV4.

(N-P) Quantification of axon length and branch points number in 2-BP-treated cortical neurons (n = 18 each concentrations).

Data are shown as means \pm s.e.m. *, $P < 0.05$; **, $P < 0.001$; ***, $P < 0.0001$; Student's t-test.

Figure S2, Related to Figure 2.

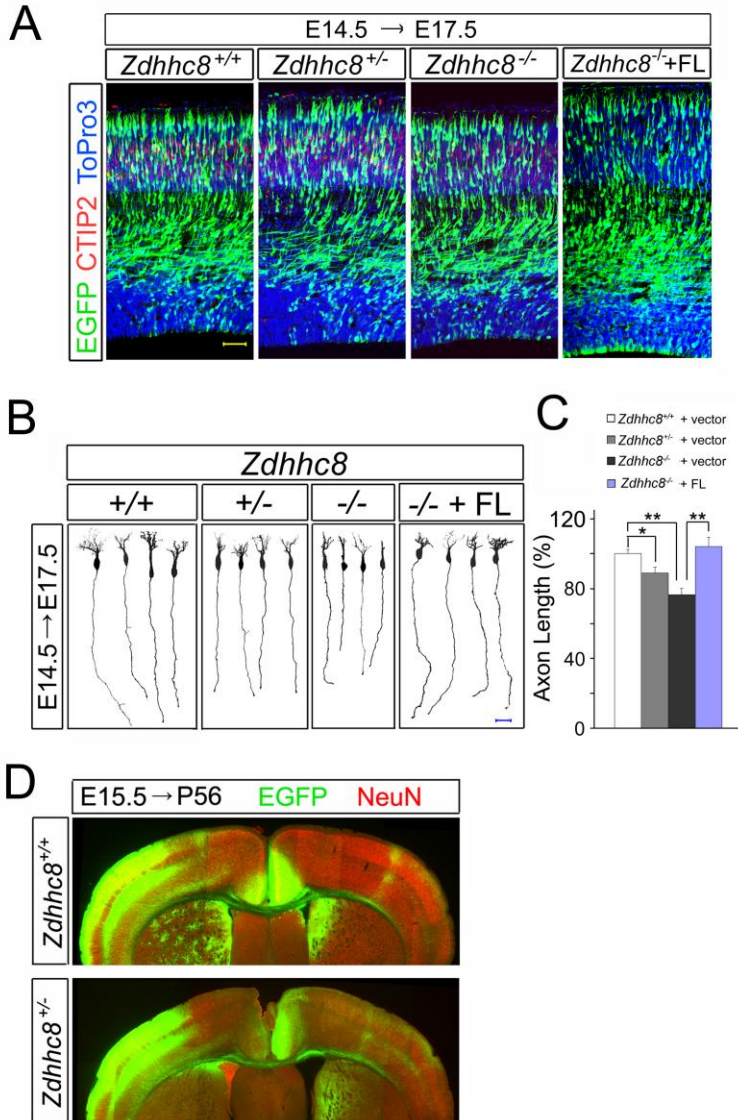


Figure S2, Related to Figure 2. Downregulation of *Zdhhc8* disrupts axonal growth *in vivo*.

(A) Confocal images of EGFP fluorescence of E17.5 mouse cortices transfected via *in utero* electroporation at E14.5. *Zdhhc8*^{-/-} cortical neurons were transfected with *IRES-EGFP* vector or *ZDHHC8FL:: IRES-EGFP* construct. Scale bar, 50 μm.

(B) Tracings of representative neurons from similar sections (A). Depicted are 2D projections of axonal arbors of neurons transfected with *IRES-EGFP* vector or *ZDHHC8FL:: IRES-EGFP* construct. Scale bar, 20 μm.

(C) Quantification of the axon length of neurons residing at the layers 2/3 reveals *Zdhhc8* deficiency results in a shortened axon and exogenous ZDHHC8FL restored axon length in *Zdhhc8*^{-/-} mice to WT levels.

(D) Representative images of EGFP-labeled neurons from coronal sections of P56 brains of *Zdhhc8* mice *in utero* electroporated at E15.5.

Data are shown as means ± s.e.m. **P* < 0.05, ** *P* < 0.001; Student's t test.

Figure S3, Related to Figure 3.

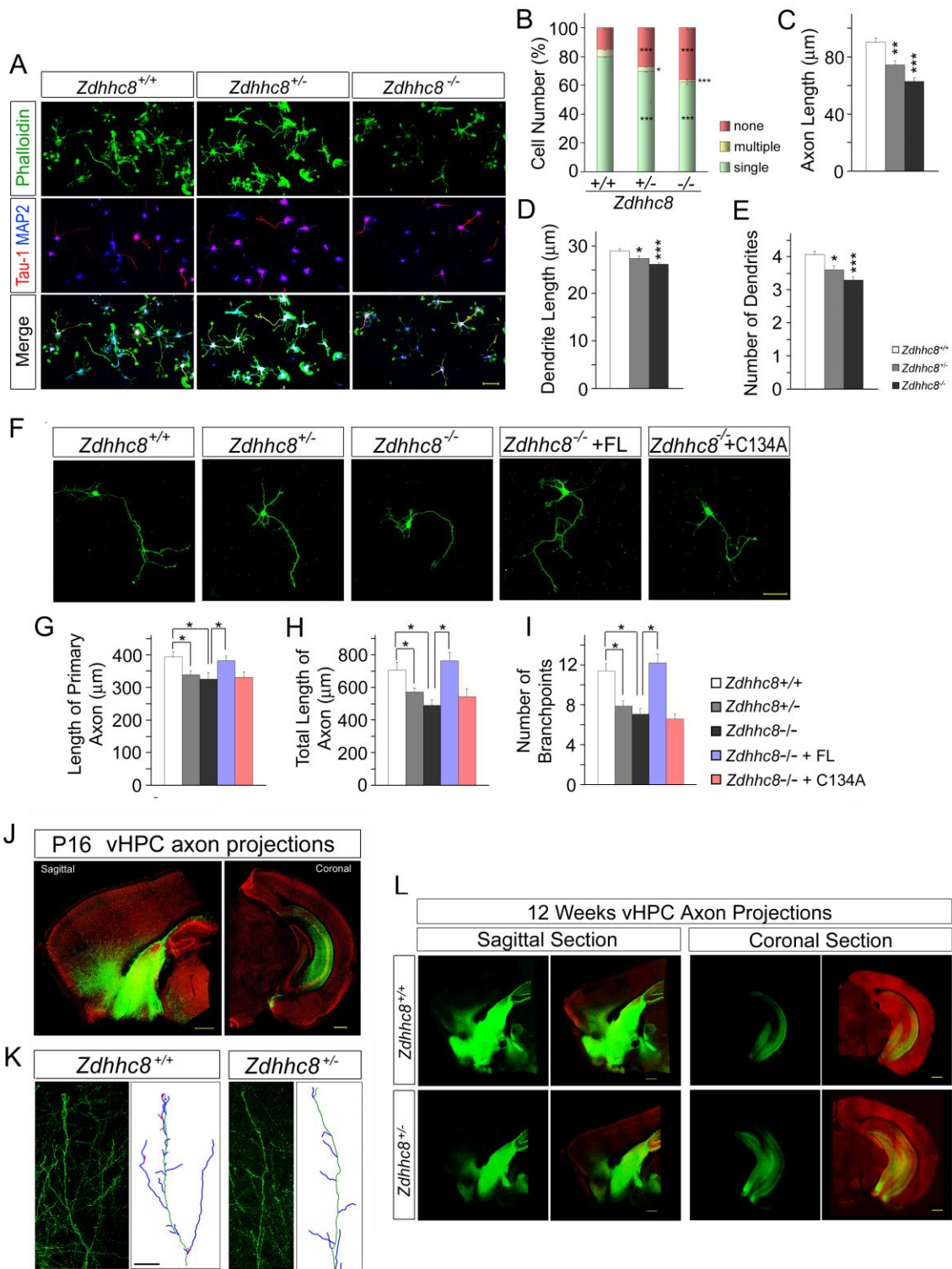


Figure S3, Related to Figure 3. Axonal alterations in *Zdhhc8*-deficient hippocampal neurons.

(A) Deficits of neuronal polarity in *Zdhhc8*-deficient hippocampal neurons at DIV3. Hippocampal neurons were immunostained with Tau-1 (*red*), MAP2 (*blue*), and phalloidin (*green*). Scale bar, 50 μ m.

(B) Quantification of the neurons, having a single (*green*), multiple (*yellow*), or none (*pink*) Tau-1-positive processes in *Zdhhc8*-deficient hippocampal cultures. 12 areas (>100 neurons/area) were analyzed for each genotype.

(C-E) Quantification of axon length, dendrite length, and dendrite number in *Zdhhc8*-deficient hippocampal neurons (> 200 neurons per each genotype).

(F) Representative images of *Zdhhc8*-dependent axonal deficits in hippocampal neurons expressing EGFP at DIV4. *Zdhhc8*^{-/-} hippocampal neurons were transfected with plasmids expressing EGFP and ZDHHC8-FL or ZDHHC8-C134A at DIV2 and fixed at DIV4. Scale bar, 50 μ m.

(G-I) Quantification of axon length and branch points number in *Zdhhc8*-deficient hippocampal neurons. Transfection of ZDHHC8-FL, but not ZDHHC8-C134A, restored axon length and branch points number. Numbers of axons analyzed: *Zdhhc8*^{+/+} transfected with an EGFP construct (n = 20), *Zdhhc8*^{+/-} transfected with an EGFP construct (n = 20), *Zdhhc8*^{-/-} transfected with an EGFP construct (n = 20), *Zdhhc8*^{-/-} transfected with EGFP and ZDHHC8-FL construct (n = 18), and *Zdhhc8*^{-/-} transfected with EGFP and ZDHHC8-C134A constructs (n = 18).

(J) Confocal images of P16 mouse brains, *in utero* electroporated with an EGFP construct to vHPC at E16.5. EGFP (*green*), NeuN (*red*). Scale bar, 500 μ m.

(K) Representative images and tracings of P16 vHPC neuron terminal branching in mPFC from similar sections as in (J). Primary (*blue*), secondary (*red*), and tertiary (*pink*) branches from axons (*green*) are highlighted. Scale bar, 50 μm .

(L) Confocal images of P84 (12 weeks) mouse brains, injected with AAV1-h-synapsin-EGFP to vHPC at P56. EGFP (*green*), NeuN (*red*). Scale bar, 500 μm .

Data are shown as means \pm s.e.m. * $P < 0.05$, ** $P < 0.001$, *** $P < 0.0001$, Student's t test.

Figure S4, Related to Figure 4.

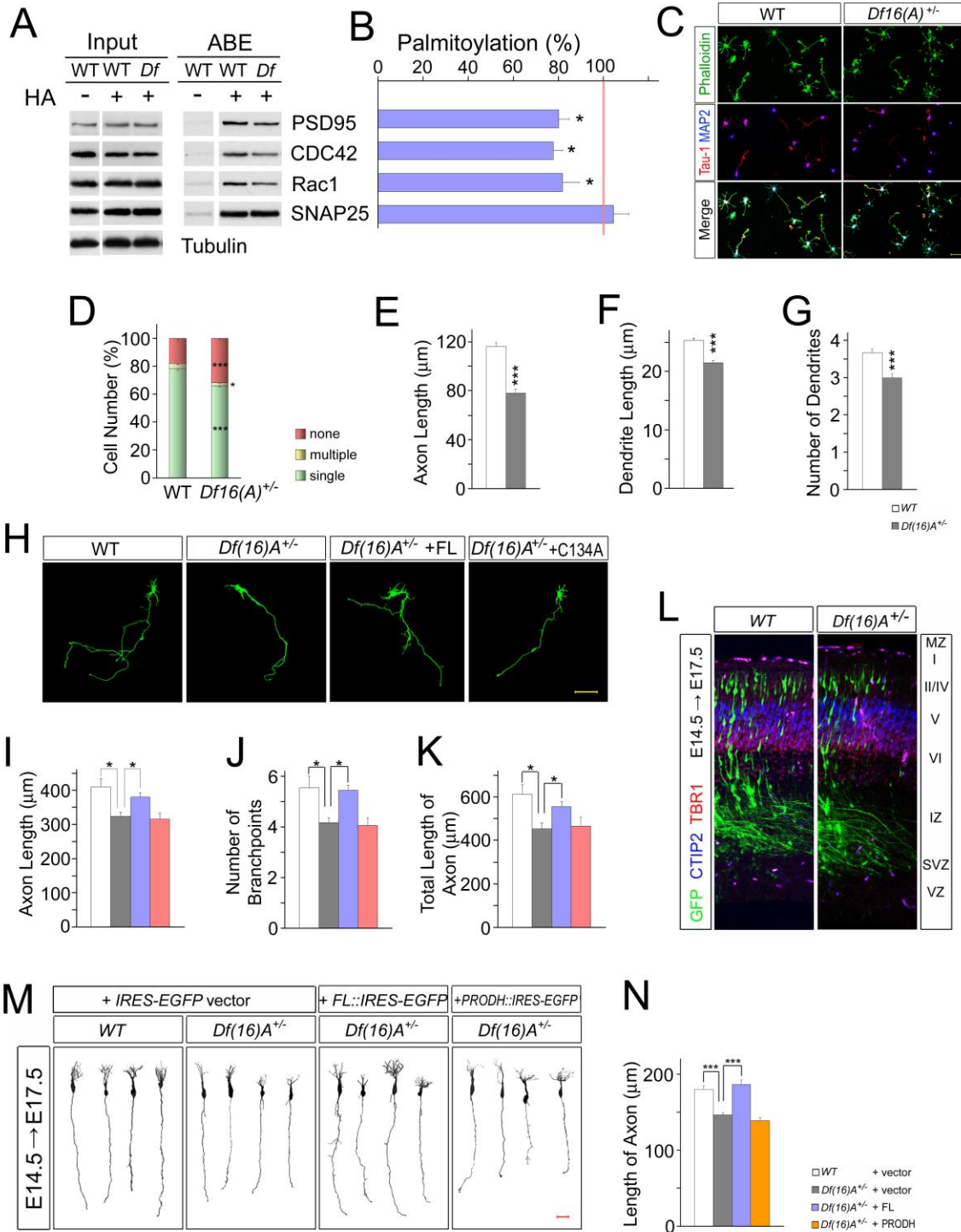


Figure S4, Related to Figure 4. ABE analysis of neuronal protein palmitoylation and axonal alterations in *Df16(A)*^{+/-} mice.

(A) Palmitoylation levels of selected candidate palmitoyl-protein substrates. Proteins, ABE-purified from cultured cortical neurons from WT and *Df16(A)*^{+/-} mice, both in the presence (+) and absence (-) of hydroxylamine (HA), were analyzed by western blotting using the indicated specific antibodies. Palmitoylated proteins are expected to show HA-dependent detection. As a control, a portion of the starting protein sample (prior to ABE purification) was also screened.

(B) Quantification of the palmitoylation changes induced by *Df16(A)*^{+/-}. Protein levels measured from the purified palmitoyl-protein samples were normalized to levels measured from the corresponding input of substrates.

(C) Deficits of neuronal polarity in *Df16(A)*^{+/-} cortical neurons at DIV3. Cortical neurons were immunostained with Tau-1 (*red*), MAP2 (*blue*), and phalloidin (*green*). Scale bar, 50 μ m

(D) Quantification of the neurons, having a single (*green*), multiple (*yellow*), or none (*pink*) Tau-1-positive processes in *Df16(A)*^{+/-} cortical cultures at DIV3. 12 areas (>100 neurons/area) were analyzed for each genotype.

(E-G) Quantification of axon length, dendrite length, and dendrite number in *Df16(A)*^{+/-} cortical neurons at DIV3 (> 200 neurons per each genotype).

(H) Representative images of *Df16(A)*^{+/-} axonal deficits in cortical neurons expressing EGFP at DIV4. *Df16(A)*^{+/-} cortical neurons were transfected with plasmids expressing EGFP and ZDHHC8-FL or ZDHHC8-C134A at DIV2 and fixed at DIV4. Scale bar, 50 μ m.

(I-K) Quantification of axon length and branch points number in *Df16(A)*^{+/-} cortical neurons at DIV4. Transfection of ZDHHC8-FL, but not ZDHHC8-C134A, partially restored axon length and branchpoints number. Numbers of axons analyzed: WT transfected with an EGFP construct

(n = 20), *Df16(A)^{+/-}* transfected with an EGFP construct (n = 20), *Df16(A)^{+/-}* transfected with EGFP and ZDHHC8-FL constructs (n = 18), and *Df16(A)^{+/-}* transfected with EGFP and ZDHHC8-C134A constructs (n = 18).

(L) Confocal images of EGFP fluorescence of E17.5 *Df16(A)^{+/-}* mouse cortices transfected via *in utero* electroporation at E14.5.

(M) Tracings of representative neurons from similar sections as in (G), depicting 2D projection of axon arbors of neurons transfected with either *IRES-EGFP* vector, *ZDHHC8FL::IRES-EGFP* or *PRODH::IRES-EGFP* constructs. Scale bar, 20 μ m.

(N) Quantification of the axon length of neurons residing at layers 2/3 reveals that presence of *Df16(A)* results in shortened axons while exogenous ZDHHC8FL restores axon length in *Df16(A)^{+/-}* mice to WT levels. Numbers of axons analyzed: WT transfected with *IRES-EGFP* vector (n = 18, 5 animals) and *Df16(A)^{+/-}* transfected with *IRES-EGFP* vector (n = 24, 5 animals), *Df16(A)^{+/-}* transfected with *ZDHHC8FL::IRES-EGFP* construct (n = 18, 4 animals) or *PRODH::IRES-GFP* (n = 27, 4 animals).

* $P < 0.05$, ** $P < 0.001$, *** $P < 0.0001$, Student's t test.

Figure S5, Related to Figure 5.

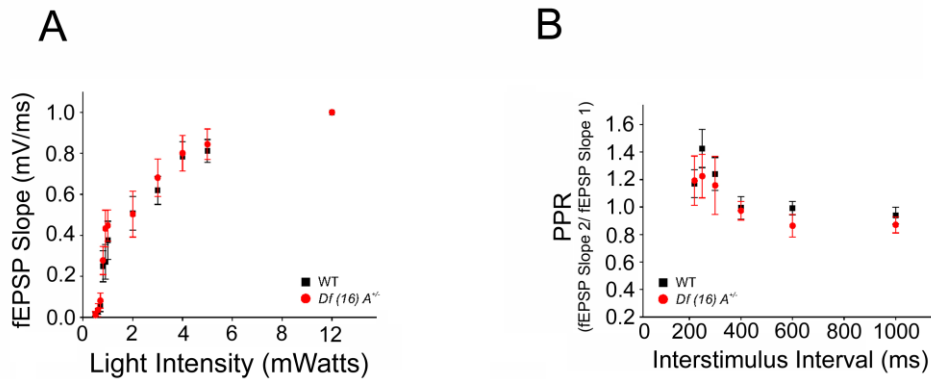


Figure S5, Related to Figure 5. Disrupted synaptic transmission in the adult brain of *Df16(A)^{+/-}* mice.

(A) The similitude of the normalized input-output curves from (Fig.5H) suggests that the L2 fibers/terminals have comparable amounts of functional ChR2 protein (Student t-tests, all intensities, $P > 0.05$).

(B) Paired-pulse ratios (fEPSP slope 2/fEPSP slope 1) of L2-L5 synapses are normal at different interstimulus intervals (two-way repeated-measures ANOVA; $P > 0.05$) in *Df(16)A^{+/-}* mice (N = 3, n = 8, red circles) compared to WT mice (N = 8, n = 17, black squares).

Data presented as means \pm s.e.m. *, $P < 0.05$.

Figure S6, Related to Figure 6.

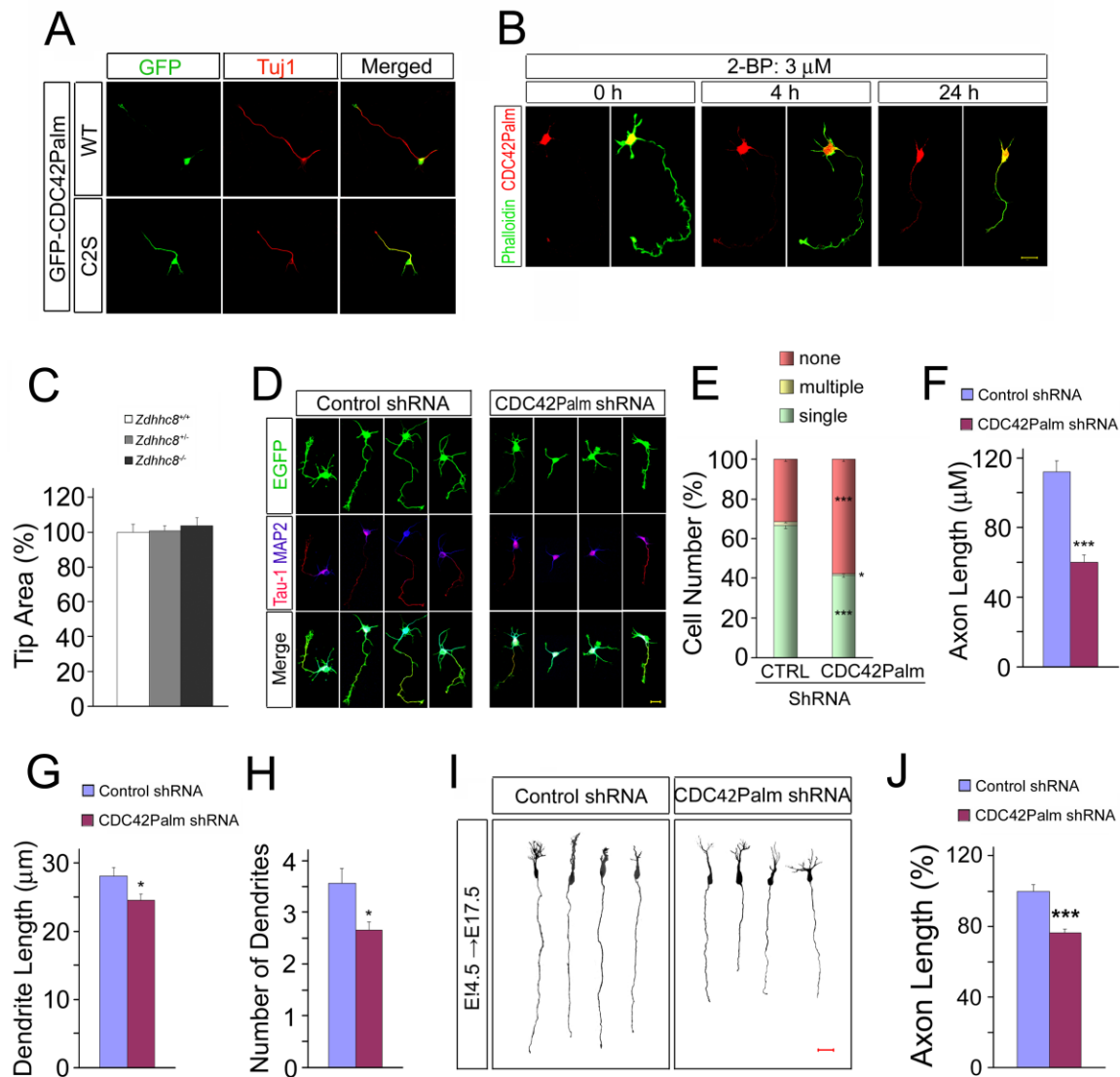


Figure S6, Related to Figure 6. Axonal alterations by knockdown of CDC42Palm.

(A) Representative images of DIV3 cortical neurons transfected with either CDC42Palm or CDC42PalmC2S (with disrupted palmitoylation sites) fused to EGFP.

(B) Effect of 2-BP on endogenous CDC42Palm localization. Cultured cortical neurons were treated with 2-BP for 4 or 24 hours and immunostained for CDC42Palm (*red*) and phalloidin (*green*).

(C) Quantification of the area of the tip of the axon in DIV3 in *Zdhhc8*-deficient neurons (*Zdhhc8*^{+/−}: n = 67, *P* > 0.5; *Zdhhc8*^{−/−}: n = 64, *P* > 0.5), compared with WT (n = 64).

(D) Representative neurons imaged at DIV3 following *ex utero* electroporation of either an shRNA targeting CDC42Palm or a control scrambled shRNA, stained with EGFP (*green*), Tau-1(*red*) and MAP2 (*blue*). Scale bar, 20 μm.

(E) Quantification of neurons with a single Tau-1-positive axon, in cortical cultures electroporated with either an shRNA targeting CDC42Palm or a control scrambled shRNA. 12 areas (> 50 neurons/area) were analyzed for each shRNA.

(F-H) Quantification of axon length, dendrite length, and dendrite number in CDC42Palm knockdown cortical neurons (n = 42), compared to control cells (n = 42).

(I) Tracings of representative neurons from coronal sections of C57 brains at E17.5, *in utero* electroporated with an shRNA targeting CDC42Palm or a control scrambled shRNA at E14.5, depicting 2D projection of axonal arbors of neurons. Scale bar, 20 μm.

(J) Quantification of the axon length of neurons residing at the layers 2/3 reveals that knockdown of CDC42Palm results in shortened axons.

P* < 0.05, ** *P* < 0.001, * *P* < 0.0001, Student's t test.

EXTENDED EXPERIMENTAL PROCEDURES

Acyl-biotinyl exchange assay. Proteins extracted from cultured mouse embryonic cortical neurons at DIV21 were analyzed by the acyl-biotin exchange assay as described with minor modifications (Wan et al., 2007). Briefly, cells from two dishes (2×10^6 cells/10 cm dish) were lysed in buffer containing 50 mM Tris (pH7.4), 5 mM EDTA, and 4% SDS, 10 mM NEM, supplemented with protease inhibitors (Complete: Rosch). Extracts were vortexed briefly and treated for 20 min at 4°C. Proteins were diluted in LB buffer (0.15 M NaCl, 50 mM Tris (pH7.4), 5 mM EDTA, 2 % Triton X-100, 10 mM NEM, protein inhibitors, and DNase, and incubated at 4 °C overnight with gentle rocking. Proteins were precipitated with chloroform/methanol, resolved with 4SB buffer [50 mM Tris (pH7.4), 5 mM EDTA, and 4% SDS], and labeled with biotin-HPDP (0.8 mM, Pierce) in buffer containing either 0.56 M hydroxylamine, pH 7.4, or 0.56 M Tris, pH 7.4, for 1 hr at room temperature. Proteins were precipitated with chloroform/methanol precipitation. Biotinylated proteins were purified with streptavidin agarose (Sigma), separated by SDS-PAGE, and analyzed by western blotting.

Expression Constructs: Human full length ZDHHC8 (ZDHHC8-FL) was cloned using reverse transcriptase PCR from a pool of human brain RNA (Mukai et al., 2004). PCR-mediated mutagenesis was utilized to generate a Cysteine to Alanine point mutant at residue 134 within the DHHC domain of ZDHHC8-FL (Mukai et al., 2008). ZDHHC8-FL and -C134A were cloned into EcoRI and BamHI sites of pcDNA3.1/myc-His(-) C (Invitrogen). pCAG-ChR2-venus, pCAG-mCherry, and pCAGIG vectors were purchased from Addgene. pCAGIG-FL were cloned ZDHHC8-FL into pCAGIG. pSuperCDC42Palm and control scrambled shRNA were gifted from Dr. Kang (Kang et al., 2008). CDC42Palm shRNA target sequence is 5'-

AGGAAGTGCTGTATATTCT. The scrambled shRNA control sequence is 5'-
AGACTCTTTCTTGCTTGT.

Antibodies

Antibodies for Western blots: The following antibodies were used: PSD95 (mouse, 1:1000, BD Bioscience), GRIP1 (rabbit, 1:1000, Upstate), SCG10 (rabbit, 1:3000, Proteintech Group), CDC42 (mouse, 1:1000, Cytoskeleton), Rac1 (mouse, 1:1000, Millipore), GAP43 (mouse, 1:4000, BD Bioscience), paralemmin (rabbit, 1:3000, gift from Dr. Manfred W. Kilimann, Uppsala University), SNAP25 (mouse, 1:3000, BD Bioscience), synaptotagmin (mouse, 1:1000, BD Bioscience), Fyn (mouse, 1: 1000, R&D system), GluR1 (rabbit, 1:1000, Upstate), Rab5 (mouse, 1:2000, BD Bioscience), α -tubulin (mouse, 1:4000, Sigma), phospho-GSK3 β (Ser9) (rabbit, 1:1000, Cell Signaling), phospho-AKT (Ser437) (rabbit, 1:1000, Cell Signaling), GSK3 β (mouse, 1: 1000, BD), AKT 1 (mouse, 1:1000 , BD Bioscience).

Antibodies for Immunocytochemistry and immunohistochemistry: The following antibodies were used: CTIP2 (rat, 1:500, Abcam), NeuN (mouse, 1:100 , Millipore), CDC42Palm (rabbit, 1: 100, gift from Dr. Kang), Tuj1 (chicken, 1:100, Neuromics), Tau-1 (mouse, Millipore, 1:300), phospho-GSK3 β (Ser9) (rabbit, 1:50, Cell Signaling), phospho-AKT (Ser437) (rabbit, 1:50, Cell Signaling), Tbr1 (rabbit, 1:200, Abcam), RFP (rabbit,1:200, Abcam), GFP (rabbit,1:200, Invitrogen), and 280GP (guinea pig, 1:100; Mukai et al., 2008). All secondary antibodies (goat, Molecular Probes) were used at 1:200 and 1:500 dilutions for immunocytochemistry and immunohistochemistry, respectively. Acti-stain 488-Phalloidin (Cytoskelton inc.) staining was performed according to a protocol provided by the company.

Western blot analysis of pAKT and pGSK3 β : Prefrontal cortices from 8 weeks mice brains were homogenized in a buffer [0.15 M NaCl, 50 mM Tris (pH7.4), 5 mM EDTA, 1% Triton X-100, complete, 100 μ M PMSF, phosphatase inhibitor II and III (Rosch). Lysates were centrifuged at 150000g and resultant supernatants were subjected to SDS-PAGE and western blot analysis. For quantitative analysis of the Western blot data, the protein band intensity was analyzed using imageJ densitometry tool. pAKT or pGSK3 β protein band intensity was normalized to AKT or GSK3 β level, respectively.

Immunocytochemistry: Primary neurons were fixed in 4% paraformaldehyde (PFA) in phosphate-buffered saline (PBS) (pH 7.4) for 10 min or 30 min (for staining with anti-Tau-1 antibody) at room temperature (RT), washed 3 times for 5 min in 1 \times PBS, permeabilized in 0.1% Triton X-100 in PBS for 5 min and washed again in PBS (3 x 5 min). Coverslips were blocked for 30 min in 3% bovine serum albumin supplemented with normalized serum and incubated for 1 hr in primary antibodies diluted into blocking buffer and washed in PBS (3 x 5 min). Prior to application of secondary antibodies, cells were blocked again in blocking buffer supplemented with 0.5M NaCl for 30 min at RT. Secondary antibodies were applied in blocking/0.5M NaCl for 30 min at RT. Following another round of washing, the coverslips were mounted onto SuperfrostPlus glass slides using Prolong Gold (Invitrogen) and stored at 4°C.

Immunohistochemistry: All the following *in vivo* experiments utilized brains from P7.5 or 12-weeks old males, perfused with PBS and 4% PFA, that were post-fixed in PFA overnight. A vibratome was used to cut 60 μ m coronal sections. Free-floating sections were blocked and permeabilized overnight at 4°C in PBTX (PBS/Triton X-100) containing 5% normal goat serum (PBTX / 5% NGS). Primary antibodies were diluted in PBTX / 5% NGS and incubated with

sections for 24 hrs at 4°C. Sections were washed overnight at 4°C in 1× PBS. Sections were incubated with secondary antibody (1:500, diluted in PBTX / 5% NGS) for 4 hrs at room temperature. Following another round of washing in 1× PBS, sections were incubated with TO-PRO3 (1:2500 in PBS) for 30 min, washed in 1× PBS (4 x 15 min), and mounted on slides using Prolong Gold (Invitrogen).

Primary neuronal cultures and Transfection: Primary cultures were prepared from cortices dissected bilaterally from E17 embryos. Cortices were individually dissociated using fire-polished Pasteur pipettes, counted, and plated in DMEM supplemented with 0.5% penicillin/streptomycin and 10% FBS. Neurons used for immunocytochemical analyses were plated on poly D-lysine coated 12 mm coverslips ($2-3 \times 10^4$ cells/coverslip), and those used in ABE labeling and western blots were plated on similarly coated 10 cm dishes (2×10^6 cells/dish). Following 3 hr incubation, the modified DMEM was replaced with neurobasal media supplemented with B27 and Glutamax (Invitrogen) in which the neurons were cultured for 2 to 21 days depending on the experiment. Post-hoc genotyping was performed on DNA extracted from tissue taken from each embryo. Transient transfections were carried out with Lipofectamine 2000 (Invitrogen) using the protocol suggested for neuronal transfection. The original supplemented neurobasal media used to culture cells prior to transfection were replaced in each well/dish following 2 hrs of incubation at 37°C with transfection reagents.

Image acquisition

Images were acquired blind to the genotype.

Image acquisition from primary neuronal cultures: Confocal images of neurons were obtained blind to genotype with the LSM510 using a Zeiss 40× objective with sequential

acquisition setting at 2048 x 2048 pixels resolution. Each image was a z series projection of approximately 6 – 9 images, and taken at 0.8 μm depth intervals using the same settings for pinhole size, brightness and contrast. To evaluate the pAKT, pGSK3 β , and CDC42Palm puncta, at least 20 neurons were analyzed from at least 6 coverslips for each genotype.

Image acquisition from tissue sections: To analyze the axon length at E17.5, images were taken with setting as z-series stacks (at 0.5 μm depth intervals) using a 20 \times Zeiss objective with constant parameters for brightness and contrast. To analyze the ipsilateral axon branch number at P7.5 and P8.5, images were taken with setting as z-series stacks (at 0.5 μm depth intervals) using 40 \times Zeiss objectives with constant parameters for brightness and contrast. To analyze the contralateral axon branch number at P8.5, images were taken with setting as z-series stacks (at 0.5 μm depth intervals) using 20 \times Zeiss objectives with constant parameters for brightness and contrast. To analyze the contralateral axon arborization at P56, images were taken with setting single scan using a 20 \times Zeiss objective with constant parameters for brightness and contrast. Similarly, to analyze the ipsilateral layer 5 axon arborization at P56, images were taken with single scan using 20 \times Zeiss objectives with constant parameters for brightness and contrast. To analyze the terminal axon branch number of ventral hippocampal neuron at P16.5, images were taken at prelimbic layer 5 in mPFC sagittal sections from *Zdhc8* mice brains, *in utero* electroporated with an EGFP construct at E16.5, using setting as z-series stacks (at 0.8 μm depth intervals) and 40 \times Zeiss objectives with constant parameters for brightness and contrast.

Image quantification

All image analysis was conducted blind to the genotype.

Quantification of neuronal polarity. To evaluate the neuronal polarity in cortical or hippocampal neuron cultures, 100-130 neurons/area were analyzed from at least 12 areas (at least 6 coverslips) derived from at least 3 embryos for each genotype and counted neurons using Tau-1 positive protrusion. Data were compared across genotypes using the Student's *t*-test. To evaluate the neuronal polarity in CDC42Palm knockdown neurons, 50-80 neurons/coverslips were analyzed from 12 coverslips transfected with EGFP plasmid-based short hairpin RNA (shRNA) targeting CDC42Palm or from 12 coverslips transfected with control scrambled shRNA. Neurons, having none, single or multiple Tau-1 positive processes were counted and data was derived from at least 3 embryos for each plasmid.

Quantification of CDC42Palm puncta. Image analysis was conducted blind to genotype as follows. CDC42Palm puncta were quantified by the immunofluorescence intensity at the tip of the longest neurite, the middle of the same process (7 μ m), and entire soma. The immunofluorescence in each image was measured by ImageJ software. All settings of threshold were maintained constant with a gain under the saturation of intensity across genotypes for each cellular region analyzed. For normalization of the tip fluorescence, signal intensity was normalized to a tip area as indicated by phalloidin. Data were compared across genotypes using the Student's *t*-test.

Quantification of pAKT and pGSK3 β puncta. Image analysis was conducted blind to genotype as follows. pAKT and pGSK3 puncta were quantified by the immunofluorescence intensity at the tip (7 μ m from the end of the process) of the longest neurite, the middle of the same process (7 μ m) and entire soma. The immunofluorescence in each image was measured by

ImageJ software. All settings of threshold were maintained constant with a gain under the saturation of intensity across genotypes for each cellular region analyzed. For normalization of the tip fluorescence, signal intensity was normalized to the tip area as indicated by Tuj1 or EGFP. Data were compared across genotypes from using the Student's *t*-test.

Quantification of axonal and dendritic morphology *in vitro*. For analysis of axon and dendrite morphology at DIV3 neurons, *z* stacks were projected maximally, and neuronal processes stained for the axonal marker Tau-1, dendritic marker MAP2, and phalloidin were traced using the overlay tools of the LSM Image Examiner 5 program (Zeiss). We chose 12 images (~ 25 cells each image) from 12 areas (at least 6 coverslips) derived from at least 3 embryos each genotype. All cells in each image were analyzed for axon length, dendrite length, and dendrite number.

For analysis of axon length and branching at DIV4 neurons, a plasmid expressing EGFP was transfected into cultures to fill the cells and facilitate visualization of all processes. *z* stacks were projected maximally, and neuronal processes stained for the axonal marker Tau-1 were traced using the overlay tools of the LSM Image Examiner 5 program (Zeiss). Neurons having a single axon were chosen. Protrusions more than 8 μm long were categorized as axon branches. The axon architecture of each neuron was also characterized by designating the order of a branch (primary, secondary and so on). Once the elaborations of the axon branch tree were outlined, branch points were counted manually, and the length of primary axon (emanating directly from the soma) and its branches were analyzed, and compared across at least three independent cultures using the Student's *t*-test. ~5 axons were traced completely in each section.

One or two of the longest axons from each coverslip were selected from the dataset and compared across at least four brains of each genotype using the Student's *t*-test.

Quantification of axonal morphology *in vivo* during development. To analyze the axonal morphology quantitatively, we performed the following procedures for each dataset obtained from the 60- μm coronal sections. To evaluate the length of axons at E17.5, EGFP-expressing neurons at CP were analyzed by projecting the *z* series and manually tracing the axon using the overlay tools of the LSM Image Examiner 5 program (Zeiss). As an indication of the effort required to trace an individual axon, typically, ~5 axons were traced completely in each section. One or two of the longest axons from each section were selected from the dataset and compared across at least four brains of each genotype using the Student's *t*-test.

For the contralateral axon terminal branching at P7.5 and P8.5, EGFP expressed axons at contralateral layer 1-4 were analyzed by projecting the *z* series and manually tracing the axon using the overlay tools of the LSM Image Examiner 5 program (Zeiss). Protrusions more than 6 μm long were categorized as axon branches. The axon terminal architecture of each neuron was also characterized by designating the order of a branch (primary, secondary and so on). Once the elaborations of the axon branch tree were outlined, branch numbers were counted manually and analyzed. We compared at least 20 axons from at least four brains of each genotype using the Student's *t*-test.

To evaluate collateral branching of ipsilateral axons at P7.5 and P8.5, EGFP expressing axons at ipsilateral layer 2-4 were analyzed by projecting the *z* series and manually tracing the axon in the layers 2/4 using the overlay tools of the LSM Image Examiner 5 program (Zeiss). Protrusions more than 6 μm long were categorized as axon branches. Once the elaborations of

the axon branch tree were outlined, branch numbers were counted manually and analyzed. We compared at least 18 axons from four brains of each genotype using the Student's *t*-test.

For rescue experiments involving ipsilateral axon collateral branching at P8.5, we electroporated an *FL:: IRES-EGFP*, *PRODH::IRES-EGFP* or a control *IRES-EGFP* vector into *Zdhhc8*-deficient mice. Branches were counted manually and analyzed. We compared at least 18 axons from four brains of each genotype using the Student's *t*-test.

For the ipsilateral axon collateral branching in CDC42Palm-knock down neurons at P8.5, we electroporated an shRNA targeting to CDC42Palm or control scramble shRNA into C57/BL6 embryos, analyzed the number of the ipsilateral axon collateral branches, and compared at least 18 axons from four brains for each shRNA using the Student's *t*-test.

To analyze the terminal axon branch number of ventral hippocampal neurons at P16.5, segments of 250-300 μm length including the primary axon terminal at prelimbic layer 5 were analyzed by projecting the *z* series and manually tracing the axon using the overlay tools of the LSM Image Examiner 5 program (Zeiss). Protrusions more than 6 μm long were categorized as axon branches. The axon terminal architecture of each neuron was also characterized by designating the order of a branch (primary, secondary and so on). Once the elaborations of the axon branch tree were outlined, branch numbers were counted manually, and branch numbers/100 μm of at least 20 axons from at least four brains of each genotype were compared using the Student's *t*-test.

Quantification of cortical axonal morphology *in vivo* in adult mice. To analyze and visualize the axon branching in adult brain, we performed the following procedures for each dataset obtained from the 60- μm coronal sections. Images acquired for the EGFP fluorescence analysis were taken with sequential acquisition setting at $2,048 \times 2,048$ pixel resolution as single image

from the frontal cortex. For the contralateral axon terminal branching at P56, the region of interest, including the strongest EGFP expressing contralateral cortical axon column in the somatosensory cortex, was defined by a 400- μ m line parallel to the each cortical layer [layer 1, layer 2/3, layer 4, layer 5, layer 6, and white matter (WM)]. The cortical layers were identified by NeuN immunostaining. The immunofluorescence in each layer was measured by ImageJ software. All settings of threshold were maintained constant across genotypes.

Callosal axons in mouse brains, *in utero* electroporated at E15.5, originate primarily from neurons of layer 2/3 of the neocortex and project homotopically to the contralateral cortex (Zhou, 2013). Transfection efficiency in ipsilateral somatosensory cortex positively correlates with immunofluorescence intensity in the contralateral axon branches ($R = 0.83$, $P < 0.0001$). Therefore, immunofluorescence intensity in the contralateral axon branches was normalized to EGFP transfection efficiency in topographically equivalent location in the ipsilateral somatosensory cortex. To quantify the transfection efficiency in the ipsilateral somatosensory cortex, images acquired for the EGFP and NeuN fluorescence analysis were taken with sequential acquisition setting at $2,048 \times 2,048$ pixel resolution as single image. The region of interest was defined by a 400- μ m line parallel to the cortical layer 2/3 in topographically equivalent location to contralateral cortical axon column. Using ImageJ cell count tool, EGFP and NeuN labeled cells were counted in the region of interest, and the frequency of EGFP – labeled cells was calculated. Sections, indicating 28-34% transfection efficiency, were analyzed for quantifications of contralateral axon branching. Data from at least 18 sections, from four brains for each genotype, were compared using the Student's *t*-test.

To analyze ipsilateral collateral axon branching at P56, images were taken with sequential acquisition setting at $2,048 \times 2,048$ pixel resolution as single image. The region of

interest was defined by a 400- μm line parallel to the each cortical layer [layer 1, layer 2/3, layer 4, layer 5, layer 6, and white matter (WM)] in topographically equivalent location to contralateral cortical axon column. The cortical layers were identified by NeuN immunostaining. The ImageJ software was used to measure the immunofluorescence in each layer. All settings of threshold were maintained constant across genotypes. Immunofluorescence intensity in the each layer was normalized to EGFP transfection efficiency in layer 2/3. Data were compared for at least 18 sections from four brains of each genotype using the Student's *t*-test.

Quantification of hippocampal-prefrontal axon morphology *in vivo* in adult mice

rAAV1/hSynapsin/EGFP was obtained from the Penn Vector Core. Viral concentration was 5×10^{12} particles per ml. For injection, mice (8 weeks) were deeply anesthetized under isoflurane and placed in a stereotaxic frame. Bregma and lambda were used for leveling and zeroing, and bilateral cranial windows were excised over vHPC, centered at -3.15mm posterior, +/- 3.15mm lateral. Virus was administered by an injection pump at a rate of 100nL/min via an elongated 10-40 μm -diameter glass micropipette. Dorsal-ventral zeroing was performed once for each hemisphere, at the most anterior-medial site. To ensure full coverage of the ventral two thirds of CA1, 200 nl were infused at each of 9 injection sites per hemisphere. Acrylic dental cement was used to cover the craniotomy after infusion. To analyze and visualize the terminal axon branching of hippocampal neuron at prelimbic prefrontal cortex in adult brain, we performed the following procedures for each dataset obtained from the 60- μm sagittal sections. Images were taken in the layer 5 of the prelimbic region of mPFC from the sagittal sections, located in the 450 μm - 650 μm lateral from the midline of the brain, with setting as z-series stacks (at 0.5 μm depth intervals) using a 63 \times Zeiss objective with constant parameters for brightness and contrast. EGFP expressing axons (80-100 μm length including the axon terminal) at prelimbic layer 5

were analyzed by projecting the z series and manually tracing the axon using the overlay tools of the LSM Image Examiner 5 program (Zeiss). Protrusions more than 6 μm long were categorized as axon branches. The axon terminal architecture of each neuron was also characterized by designating the order of a branch (primary, secondary and so on). Once the elaborations of the axon branch tree were outlined, branch numbers were counted manually, and at least 20 axons, from four brains, for each genotype were compared using the Student's t -test.

Electrophysiology and frontal cortex slice preparation. Channel rhodopsin2-venus and mCherry constructs were *in utero* electroporated to dorsolateral cortex at 16.5 embryos. Experiments were carried out on P50-P60 mice. Mice were anesthetized with Isoflurane and rapidly decapitated. Then, the brain was removed and placed in ice-cold dissecting solution (in mM): sucrose (195), NaCl (10), KCl (2.5), NaH_2PO_4 (1), NaHCO_3 (25), glucose (10), MgSO_4 (4), CaCl_2 (0.5). The cerebellum was removed and coronal brain sections were cut on a vibratome (Leica VT1200S). The freshly cut frontal cortex coronal slices (immediately rostral to the dorsal hippocampus) were transferred to an interface chamber and allowed to recover for 2 hours at 34–36 °C. During the recordings, the slices were continuously perfused with artificial cerebrospinal fluid (aCSF) (bubbled with 5% CO_2 /95% O_2) that had the following composition (in mM): NaCl (124), KCl (2.5), NaH_2PO_4 (1), NaHCO_3 (25), Glucose (10), MgSO_4 (1), CaCl_2 (2). The aCSF was maintained at 34 to 36 °C and fed by gravity at a rate of ~2 ml per minute.

Field EPSPs (fEPSPs) were recorded via a glass microelectrode (3–5 $\text{M}\Omega$) filled with aCSF and placed in layer 5 of the frontal cortex (500 μm from dorsal surface, in a region ~45° from the midline). The fEPSPs were evoked using photostimulation with a blue laser (473 nm, OEM Laser Systems). Blue light was delivered using a fiber optic mounted on a micromanipulator and placed in close proximity to the recording electrode in layer 5. Basic synaptic transmission was

assessed at 0.033 Hz, with stimulation intensities increasing from 0.5 to 10 mWatts (pulse duration = 1 ms). The subsequent experiments were performed at the stimulus intensity that generated a fEPSP one-third of the maximum fEPSP obtained at maximum light intensity (10 mWatts). Vesicle release probability was assessed using a paired-pulse protocol with interstimulus intervals of 20, 50, 100, 200, 400, and 800 ms. Signals were acquired using the pClamp10 software, the Digidata 1440A (Molecular Devices) and an extracellular amplifier (Cygnus Technologies). The fEPSP were quantified by measuring the initial slope of the peak negativity of the synaptic responses. Statistical analyses were done using the Sigmaplot and Prism softwares. A t-test or a two-way repeated-measures ANOVA was used to compare differences between genotypes. A confidence level of $P < 0.05$ was considered statistically significant. Data are presented as mean \pm SEM. N indicates number of animals, n indicates number of slices. All recordings and the majority of data analysis were done blind to the genotype.

Behavior and field potential analysis: Three- to 6-month-old mice were anesthetized with isoflurane (Butler Schein, Chicago, IL) and placed in a stereotaxic head holder. A bundle of 13 twisted-wire stereotrodes (12.5 μ m) were implanted in the mPFC (1.6 mm anterior to bregma, 0.3 mm lateral to midline, 1.4 mm below brain surface) and single tungsten wire field electrodes (75 μ m) were implanted in the dHPC (1.94 mm posterior, 1.5 mm lateral, 1.4 mm ventral) and the vHPC (3.16 mm posterior, 3.0 mm lateral, 4.0 mm ventral). Skull screws were attached above the frontal cortex and cerebellum served as ground and reference, respectively. Animals were trained on a non-match to sample T-maze task. The behavior protocol began with 2 days of habituation during which animals freely explored the maze for 10 minutes, followed by 2 days of

shaping when animals were required to alternate between goal arms of the maze to receive food rewards. After shaping was completed, training and testing sessions were conducted. Each trial of the task consisted of a sample and choice phase. In the sample phase, a mouse ran down the center arm of the maze and was directed into one of the goal arms. The mouse returned to the start box where it remained for a delay of 10 seconds. In the choice phase, the mouse was required to select the arm opposite to that visited in the sample phase to receive a reward. Animals were given daily training of 10 trials until they reached criterion performance, defined as performance of at least 70% correct per day for 3 consecutive days. After criterion was reached, animals completed daily testing sessions composed of 20-25 trials. Local field potentials were recorded throughout the experiment. The coherence of field potential was computed with the “mscohere” function in Matlab (MathWorks, Natick, MA). Theta coherence was computed as the mean coherence in the 4–12-Hz range. To measure the correlation between baseline theta coherence and days to reach criterion performance, coherence was computed from neural activity recorded during a habituation session before the initial training session. Only neural data during periods of continuous movement (velocity between 5 and 25 cm/s) were used to compute theta coherence.

Supplementary References

Saito, T. (2002). In vivo electroporation in the embryonic mouse central nervous system.

Nat Protoc. *1*, 1552-1558.

Zhou, J., Wen, Y., She, L., Sui, Y.N., Liu, L., Richards, L.J., and Poo, M.M. (2013). Axon position within the corpus callosum determines contralateral cortical projection. *Proc. Natl. Acad. Sci. U. S. A.* *110*, 2714-2723.